Scanning tunneling spectroscopy study of Cu(554): Confinement and dimensionality at a stepped surface

M. Hansmann,[1] J. I. Pascual,[1,2] G. Ceballos,[1,3] H.-P. Rust,[1] and K. Horn[1]

[1]*Fritz-Haber-Institut der Max-Planck-Gesellschaft, Faradayweg 4–6, 14195 Berlin, Germany*
[2]*Instituto de Ciència de Materials de Barcelona, CSIC, 08193 Bellaterra, Spain*
[3]*Laboratorio Nazionale TASC-INFM, 34012 Trieste, Italy*

Electronic structure investigations of Cu(554) using low-temperature scanning tunneling microscopy/spectroscopy indicate that the dimensionality of the (111)-derived surface state changes from two dimensions to one dimension when the electron energy and wave vector comply with the lateral confinement conditions of the individual terrace. Moreover, an alternative explanation can be given for the gradual changeover from terrace to step modulation with an increasing miscut angle reported in earlier photoemission experiments.

Vicinal surfaces have been extensively studied in recent years. They act as templates for growing one-dimensional (metal) structures, since they alter the adsorption modes compared to low-index surfaces.[1–3] Beyond this merely functional approach, the clean surface itself has intriguing electronic properties. The regular step array induced by a small-angle miscut gives rise to an additional periodicity in one dimension, the step superlattice, which may influence the surface electronic structure.

Noble-metal surfaces are most suitable for studying the effects of this superlattice due to the free-electron-like behavior of the surface states of their low-index faces. Previous photoemission experiments on vicinal copper surfaces have revealed indications of one-dimensional states[4–6] as well as shifts in the surface state because of the reduced size of the Brillouin zone.[7,8] Moreover, the electronic properties can be tuned by choosing an appropriate miscut angle. Ortega *et al.*[9,10] found for vicinal Cu(111) surfaces that the surface-state band minimum shifts gradually from the (111) terrace normal direction to the vicinal surface normal direction as the miscut angle becomes larger than a critical angle. This was interpreted as a coupling of the surface state to the bulk states via the reciprocal superlattice vector, leading to a surface resonance bound by the potential of the average surface.[10]

In this work, the electronic structure of Cu(554) was studied by means of scanning tunneling microscopy/spectroscopy at low temperature. This technique allows to locally acquire electronic structure data on individual terraces and sites rather than averaging over the entire sample as in photoemission. The results show that the surface electronic states are strongly affected by local confinement to (111) terraces leading to a reduced dimensionality.

The Cu(554) sample was cut from a Cu(111) crystal with an angle of $5.7°$. It has an average terrace width of 21 Å or nine atomic rows [Fig. 1(a)]. The steps are perpendicular to the $[11\bar{2}]$ direction featuring (111)-like facets. The crystal was prepared by repeated Ar$^+$ sputtering/annealing (around $550°C$) cycles, and was subsequently transferred to a home-built ultrahigh vacuum scanning tunneling microscopy (STM) working at ~ 5 K.[11] As such low temperatures, the STM provides a high-energy resolution (≈ 2 meV) as well

as high mechanical stability which is needed for long recording times. Moreover, the frizzy appearance of the Cu steps due to the mobility of step atoms at room temperature[12] induced by the tip[13,14] is frozen out. A lock-in technique is used to acquire the differential conductance (dI/dV) signal, which is thought to be related to the local density of states (LDOS).[15] The sample bias voltage V_s is equivalent to the energy relative to the Fermi energy.

In the STM images, the Cu(554) surface consists of a fairly regular array of (111) terraces where the average terrace width is in good agreement with the miscut angle [Fig. 1(b)]. However, deviations are observed and terrace widths are distributed around the expected width of 21 Å. Moreover, kink sites are present, affecting the step superlattice geometry.

In Fig. 2(a), the dI/dV spectrum of an exceptionally wide (225 Å) terrace is shown, together with that of three narrower terraces. Each curve represents an average of many
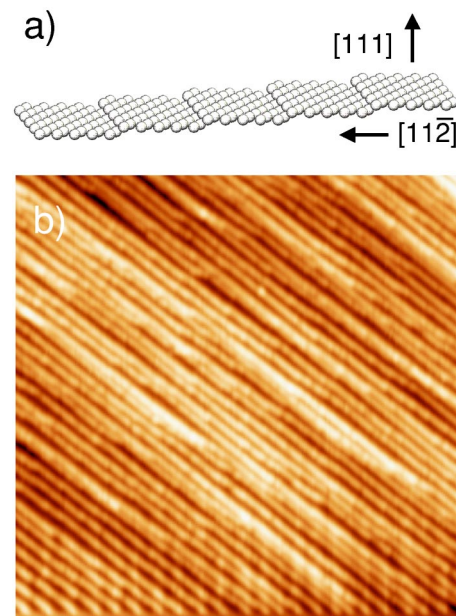

FIG. 1. (a) Atomistic model of the Cu(554) surface. Every (111) oriented terrace is 21 Å wide and consists of nine atomic rows. (b) Topographic image of the Cu(554) surface. 810×810 Å^2. $V_s = 400$ mV, $I = 0.6$ nA.
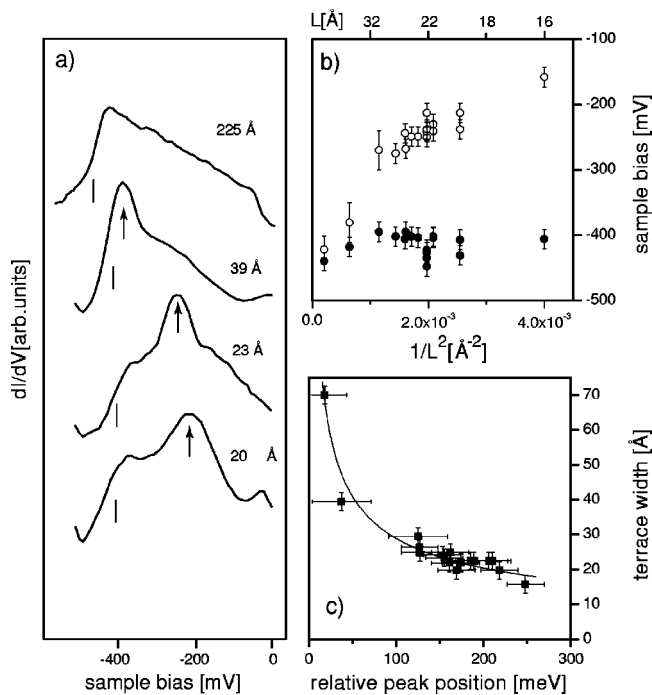
FIG. 2. (a) dI/dV spectra taken on terraces of different widths as indicated on the right-hand side. Straight lines denote the onset position taken from the numerical point of inflexion. Peaklike features on narrower terraces are marked with an arrow. (b) Energies of onsets (closed circles) and peaks (open circles) taken from spectra similar to those in Fig. 1(a). (c) Peak energy relative to their individual onsets in (b) plotted against the step width. The fit corresponds to a finite 1D potential well with the barrier height as the fit parameter.

spectra taken on the same terrace to exclude the influence of local effects. The sudden onset of an increase of the dI/dV signal is interpreted as due to the surface state. On the wide terrace, the onset is the sole visible feature and appears at around (-445 ± 15) mV, in agreement with flat Cu(111) STM measurements[16–18] as well as photoemission spectroscopy (PES) studies.[19] A close analysis of the onset width can provide the lifetimes of surface states.[18]

In the spectra of the narrower terraces, two aspects are important. First, the onset is shifted upwards by about (50 ± 10) mV compared to the wide terrace; for the two largest terraces, the onset shifts towards the (111) onset value of -445 mV. Second, a broad but very distinct peak appears, depending on the terrace width L. The behavior of both characteristics is presented systematically in Fig. 2(b), where the energies of onset and peak are plotted vs. the inverse square terrace width $1/L^2$ for many terraces (see below). The shift of the onset [relative to the flat Cu(111) surface state] remains fairly constant for all narrow terraces while the peak shows a strong dependence on terrace width.

The onset shift reflects the behavior of the average (554) surface. In earlier room-temperature STM studies[8] an increasing shift of the surface-state onset of vicinal Cu(111) surfaces with increasing miscut angle was found. This energy shift was interpreted in terms of a one-dimensional (1D) Kronig-Penney model.[20] Here, the shift is an indication that the Cu(111) extended 2D surface state still exists on this

stepped surface,[9] only partially affected by the finite transparency of the step superlattice. Using the Kronig-Penney model, we determine the transmission coefficient $|T|^2$ and the phase shift ϕ of the transmitted wave at vicinal steps. Applying this approach to Cu(554) with a terrace width of 21 Å and an onset shift of 50 meV, we obtain $|T|^2=0.48$ and $\phi=-0.26\pi$. Moreover, the potential barrier parameter $U_0 b$ is found to be 1.35 eV Å.

The second feature in the spectra, i.e., the peak, only occurs on narrow terraces. As calculated previously[20] for a regular step lattice, the Kronig-Penney model predicts the opening of a small gap at the boundary of the superlattice Brillouin zone, which is then accompanied by a sudden increase in the LDOS arising from the singularity at the gap edge. Because the gap arises from the collective coupling of terraces giving rise to the "superlattice," it should appear at the same energy for all terraces. In the experiments, however, the peak energy shows a clear dependence on terrace width, and one can observe shifts of the peak position even at adjacent terraces with different widths. Thus, a different interpretation must apply here to explain the structure found in the LDOS. Such peaks are usually characteristic of electronic states whose dimensionality is reduced, as we suggest, states confined laterally by the step potential.[9,21] For such confined states, we expect that they are no longer exposed to the extended superlattice potential; instead, their properties are determined by local confinement on a single terrace.

The energy dependence of the peak feature on $1/L^2$ [Fig. 2(b)] demonstrates a "particle in a box" picture. For the simple case of infinitely high potential walls, the lowest confined state exhibits the energy $E=\hbar^2 k^2/(2m^*)$ $=\hbar^2\pi^2/(2m^*L^2)$, where k is the wave vector and m^* is the effective mass. More accurately, the data can be fitted using a finite 1D potential square well model by taking the relative energy of each peak to its surface-state onset [see Fig. 2(c)]. The fitted energy barrier height suggests total confinement. This result is in contrast to our previous analysis of the onset shift pointing to a rather transparent well. In the related case of stepped Au(111) surfaces,[22] photoemission studies were interpreted in terms of total confinement. After all, our analysis shows that the peak "state" contributes strongly to the electronic surface structure of Cu(554).

That the dimensionality of surface states on this vicinal surface is reduced from two dimensions can be directly seen from the study of scattered surface electrons. Electronic states in the vicinity of a defect form standing wave patterns due to coherent interference. Conductance (i.e., dI/dV) images resolve oscillations related to the LDOS standing waves at the energy eV_s relative to the Fermi energy, where V_s is the sample bias voltage, though deviations especially close to the scatterer might occur.[23] By intentionally touching the sample with the tip, we have created steps at an angle of 120° relative to the vicinal (111) steps [Fig. 3(a)], which act as the scatterer in the experiment. Figure 3(b) shows a conductance image at $V_s=-57$ mV. Because of the vicinal step superstructure, the oscillations are only clear along the narrow (111) terraces [cf. Fig. 3(b)]. Performing a line scan along the terraces, we take a spectrum at each point of the scan to achieve spatial resolution of the electronic structure
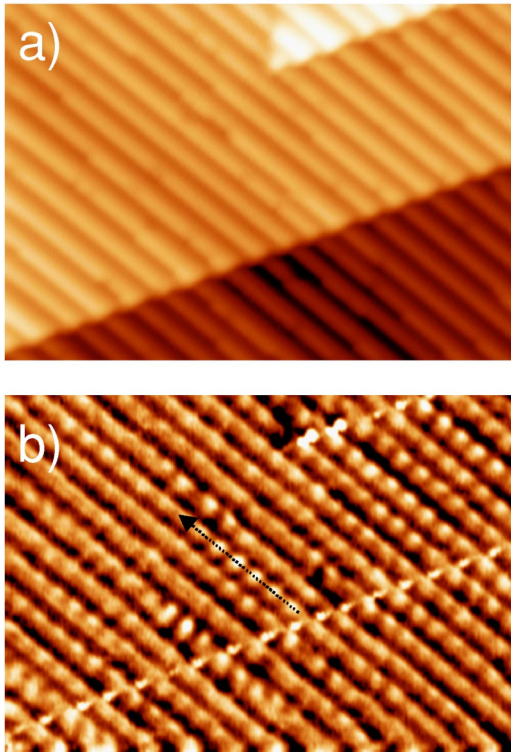
FIG. 3. (a) Surface topography after a deliberate tip crash in the vicinity of the image. Besides the (111) step edges running from top left to bottom right (due to the miscut), there are also steps of the (554) surface at an angle of 120°. These steps are used as scatterers. Image is 440×310 Å^2. $V_s=-380$ mV, $I=5.8$ nA. (b) Conductance image of the same area as in (a) at $V_s=-57$ mV. The feedback was active and adjusted to a low time constant compared to the period of the lock-in frequency($f=2141$ Hz), to ensure that the modulation voltage causes only a current modulation. Standing waves appear as spherical protrusions in this image due to the vicinal step superstructure. The arrow marks the direction in which the dispersion of the waves is determined for various energies.

data. As one sweeps through the energies, the dispersion of the corresponding state is determined from the oscillations by performing a 1D Fourier transform (FT) in the direction of measurement (i.e., along the terraces).[24,25] The result for energies below the Fermi level is represented in Fig. 4. The dispersion of the state is found to exhibit a free-electron-like behavior. By fitting a parabola to the gray scale maxima, the effective mass was found to be $m^*=0.45\ m_e$.

We use this finding to solve a problem arising from the rather complicated vicinal surface morphology of Cu(554). Due to the spherical structure of conductance image protrusions in Fig. 3(b), it cannot be distinguished whether (i) scattered electron waves propagate normal to the scattering step or (ii), alternatively, are confined to run along the (111) terraces, where the vicinal steps act as a kind of waveguide. However, the choice of the accurate scattering geometry will determine the outcome of the FT analysis. If case (ii) is true, we find the real effective mass in the FT, since the direction of the line scan used for the dispersion measurement and the wave vector of the backscattered electrons coincide. If case (i) is true, measurement direction and wave vector include an
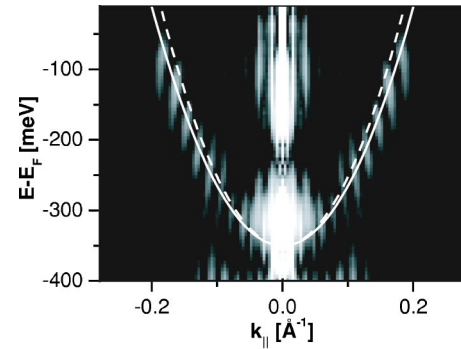

FIG. 4. 1D Fourier transform of the energy dispersion along the terrace direction. The parabolic shape reflects the free-electron-like behavior of the noble-metal surface state. The straight parabola is the fit for terrace confinement in good agreement with the data. The dashed line shows a parabola assuming delocalized electrons. Vertical lines close to the center of the image ($k=0$) are due to the limited size of the real-space scan.

angle of 60°. For this reason, the FT would not show the true band structure because a projected, too large wavelength leads to a too small effective mass in reciprocal space. To rule in favor of (i) or (ii), an identical FT analysis of wave patterns was performed on an exceptionally wide terrace, and in a separate experiment on a Cu(111) surface. In both cases, the effective mass from the FT analysis of $m^*=0.45\ m_e$ was found to be in good agreement with the high-resolution PES result of $0.41\ m_e$.[19] Photoemission studies on Cu(332) show that the effective mass on a vicinal surface remains unaffected perpendicular to the step superlattice.[4] We conclude that we have chosen the right scattering geometry (ii) because of the excellent agreement between m^* on Cu(111) and Cu(554). Physically, this means that surface electrons are really confined on the (111) terraces rather than being delocalized on the average (554) surface, in consistency with the analysis of dI/dV spectra.

In conclusion, our results indicate an energy and terrace width dependent modification of the Cu(111) surface state induced by the step superlattice. Just at and above the bottom of the band, the surface state exhibits a two-dimensional character since the energy of the onset is the same for all terraces on the surface. As soon as electrons comply with the resonance conditions of the quantum well, formed by an individual terrace, (i.e., with terrace width being a half integer of the electron wavelength), their propagation is locally confined. Simple model calculations show that even for the non-bound, scattered states, the reflectivity of a 1D well is distinctly increased whenever electrons match the resonance condition.[26] For the superlattice, it means that the coupling between terraces is reduced. The fact that the wave patterns are confined to the terraces further demonstrates that the electronic structure is dominated by this primarily one-dimensional behavior. For a perfectly regular step superlattice, one also expects an increase in the LDOS at the energy of the quantum well resonant wave vector which is then equivalent to the Brillouin-zone boundary of the superlattice in the reciprocal space.[20] Whether the terrace width dependence that we see in our experiment has to be understood in

terms of deviations from this superlattice or as an independent, fully local effect, cannot be determined as yet.

A continuous transition in dimensionality has been reported for the Si(111)−(5×2)−Au system,[27] where the gold atoms form atomic chains on the stepped silicon substrate. Here, on vicinal Cu(111) surfaces, the dimensionality can be tuned by choosing an appropriate miscut angle, as the gradual switchover from terrace to step modulation observed by Ortega et al.[9] suggests. In their work, this switchover occurs at critical miscut angle of 7° (17 Å terrace width). At this angle, the gap of the Fermi surface around L projected onto the misoriented surface closes, effectively turning the surface state into a surface resonance.[10] This electronic crossover was interpreted as a displacement of the weight of the electronic wave function deeper into the bulk, increasing the transparency of the step potential barrier.[28]

On the vicinal Cu(111) surface with the critical miscut angle of 7°, the bottom of the surface state band is shifted upwards[10] to −290 meV [Cu(554): −400 meV]. Taking the average terrace width of 17 Å into account, the lowest confined state above this onset appears at the Fermi energy. This means that no occupied states due to confinement on individual terraces can exist at larger miscut angles and therefore contribute to the photoemission signal. Our results show that confinement strongly increases the LDOS at the energy of the confined state. In the absence of local confinement, the much weaker contribution of the overall, Kronig-Penney-like effect dominates. This might explain why no terrace-bound surface band was found for larger miscut angles in the PES experiments. It has to be stated that Cu(554) features (111)-like steps instead of the (100)-like used by Ortega et al. However, in the case of Ag(111) it was shown that both types of steps have identical scattering properties.[21]

The geometry of the surface (i.e., the terrace width) affects the surface electronic structure by shifting the position of the confined or quantum-well states (QWS's) relative to the Fermi energy. The interplay of surface morphology and QWS energies was found in various systems exhibiting such interesting phenomena as preferred or "magic" film thicknesses.[29–31]

In summary, the electronic structure of vicinal Cu(111) surfaces shows a two-dimensional behavior for low energies just above the onset of the surface state, whereas confinement to terraces dominates the electronic structure at higher energies. These confined states may play an important role in the transition from the (111) terrace-bound surface state to a resonance of the vicinal surface found in photoemission experiments.

---

[1] K.N. Altmann, J.N. Crain, A. Kirakosian, J.-L. Lin, D.Y. Petrovykh, F.J. Himpsel, and R. Losio, Phys. Rev. B **64**, 035406 (2001).

[2] P. Gambardella, M. Blanc, H. Brune, K. Kuhnke, and K. Kern, Phys. Rev. B **61**, 2254 (2000).

[3] T. Jung, R. Schittler, J.K. Gimzewski, and F.J. Himpsel, Appl. Phys. A: Mater. Sci. Process. **61**, 467 (1995).

[4] F. Baumberger, T. Greber, and J. Osterwalder, Phys. Rev. B **62**, 15 431 (2000).

[5] X.J. Shen, H. Kwak, D. Mocuta, A.M. Radojevic, S. Smadici, and R.M. Osgood, Jr., Phys. Rev. B **63**, 165403 (2001).

[6] J.E. Ortega, F.J. Himpsel, R. Haight, and D.R. Peale, Phys. Rev. B **49**, 13 859 (1994).

[7] X.Y. Wang, X.J. Shen, and R.M. Osgood, Jr., Phys. Rev. B **56**, 7665 (1997).

[8] O. Sánchez, J.M. García, P. Segovia, J. Alvarez, A.L. Vázquez de Parga, J.E. Ortega, M. Prietsch, and R. Miranda, Phys. Rev. B **52**, 7894 (1995).

[9] J.E. Ortega, S. Speller, A.R. Bachmann, A. Mascaraque, E.G. Michel, A. Närmann, A. Mugarza, A. Rubio, and F.J. Himpsel, Phys. Rev. Lett. **84**, 6110 (2000).

[10] J.E. Ortega, A. Murgarza, A. Närmann, A. Rubio, S. Speller, A.R. Bachmann, J. Lobo, E.G. Michel, and F.J. Himpsel, Surf. Sci. **482-485**, 764 (2001).

[11] H.-P. Rust, J. Buisset, E.K. Schweizer, and L. Cramer, Rev. Sci. Instrum. **68**, 129 (1997).

[12] J. Frohn, M. Giesen, M. Poensgen, J.F. Wolf, and H. Ibach, Phys. Rev. Lett. **67**, 3543 (1991).

[13] J. Li, R. Berndt, and W.D. Schneider, Phys. Rev. Lett. **76**, 1888 (1996).

[14] F. Mugele, A. Rettenberger, J. Boneberg, and P. Leiderer, Surf. Sci. **377-379**, 62 (1997).

[15] R.S. Becker, J.A. Golovchenko, D.R. Hamann, and B.S. Swartzentruber, Phys. Rev. Lett. **55**, 2032 (1985).

[16] M.F. Crommie, C.P. Lutz, and D.M. Eigler, Nature (London) **363**, 524 (1993).

[17] L. Bürgi, Dissertation, EPF Lausanne (1999).

[18] J. Kliewer, R. Berndt, E.V. Chulkov, V.M. Silkin, P.M. Echenique, and S. Crampin, Science **288**, 1399 (2000).

[19] F. Reinert, G. Nicolay, S. Schmidt, D. Ehm, and S. Hüfner, Phys. Rev. B **63**, 115415 (2001).

[20] L.C. Davis, M.P. Everson, R.C. Jaklevic, and W. Shen, Phys. Rev. B **43**, 3821 (1991).

[21] L. Bürgi, O. Jeandupeux, A. Hirstein, H. Brune, and K. Kern, Phys. Rev. Lett. **81**, 5370 (1998).

[22] A. Mugarza, A. Mascaraque, V. Pérez-Dieste, V. Repain, S. Rousset, F.J. García de Abajo, and J.E. Ortega, Phys. Rev. Lett. **87**, 107601 (2001).

[23] J. Li, W.D. Schneider, and R. Berndt, Phys. Rev. B **56**, 7656 (1997).

[24] L. Petersen, P.T. Sprunger, P. Hofmann, E. Lægsgaard, B.G. Briner, M. Doering, H.-P. Rust, A.M. Bradshaw, F. Besenbacher, and E.W. Plummer, Phys. Rev. B **57**, R6858 (1998).

[25] J.I. Pascual, Z. Song, J.J. Jackiw, K. Horn, and H.-P. Rust, Phys. Rev. B **63**, 241103(R) (2001).

[26] M.D. Stiles, Phys. Rev. B **48**, 7238 (1993).

[27] R. Losio, K.N. Altmann, and F.J. Himpsel, Phys. Rev. Lett. **85**, 808 (2000).

[28] J.E. Ortega, A. Mugarza, V. Repain, S. Rousset, V. Pérez-Dieste, and A. Mascaraque, Phys. Rev. B **65**, 165413 (2002).

[29] J.J. Paggel, T. Miller, and T.-C. Chiang, Science **283**, 1709 (1999).

[30] W.B. Su, S.H. Chang, W.B. Jian, C.S. Chang, L.J. Chen, and T.T. Tsong, Phys. Rev. Lett. **86**, 5116 (2001).

[31] R. Otero, A.L. Vázquez de Parga, and R. Miranda, Phys. Rev. B **66**, 115401 (2002).